PI-Funnel Control for Two Mass Systems

Achim Ilchmann and Hans Schuster

***Abstract*—We control a two mass system with uncertain parameter values, encompassing friction and hysteretic effects, modelled as a functional differential equation. As opposed to control strategies invoking identification mechanisms or neural networks, we propose controllers relying on structural system properties only. Output behaviour with prespecified accuracy is guaranteed by the funnel controller, active damping of the shaft oscillation by the high-pass filter, zero tracking output error in the steady state by the PI-controller and bounded input disturbances are rejected. Finally, the controllers are implemented on a real plant, an electrical drive.**

***Index Terms*—Adaptive control, electric drives, tracking, two mass systems.**

I. Introduction

We control an uncertain nonlinear two mass system modelled as a single-input, single-output functional differential equation. It is a three dimensional linear equation perturbed by a functional operator, see (1) and Fig. 2, modelling nonlinear friction, hysteretic effects, dead zone effects and others. A prototypical example of a nonlinear two mass system is the test rig depicted in Fig. 1. The driving machine provides a torque which is transmitted to the load by an elastic shaft; the second machine emulates the behaviour of the load. Since every real shaft is flexible, perturbations may excite oscillations. Those have to be damped by injecting a suitable driving torque such that the load-speed converges to a given reference signal.

Generally, the parameters of real plants are not known precisely. If these uncertainties and nonlinear effects are negligible, LTI-approaches are applicable and find a widespread use in industrial applications; see [3] and the references therein. It has been observed in [2] that identification and compensation for friction together with LTI-approaches gives insufficient control performance in case of a small mass moment of inertia. Additionally, controllers, based on identification mechanisms, neural networks or fuzzy methods [3], are highly complex. The concept of funnel controller, introduced by [5] (for a history of high-gain control and applications of the funnel controller see [7]), is based on structural properties of the system only such as stable zero dynamics, relative degree one and known sign of the high-frequency gain. It obeys prespecified transient behaviour, tolerates measurement noise and nonlinear dynamic disturbances. However, the practical drawbacks of the funnel controller are that a non-zero steady state error usually remains and oscillations in the elastic shaft are not damped. Both drawbacks are overcome in the present technical note by combining the funnel controller with a PI-controller and a high pass filter, see Fig. 2; this had been suggested and drafted by Schuster *et al.* [9]. Moreover, we include input disturbances, a fairly large class of nonlinearity in the model and test all controllers on a real plant, an electric drive.

Manuscript received September 23, 2008; revised November 25, 2008. Current version published April 08, 2009. Recommended by Associate Editor C.-Y. Su.

A. Ilchmann is with the Institute of Mathematics, Technical University Ilmenau, Ilmenau 98693, Germany (e-mail: achim.ilchmann@tu-ilmenau.de).

H. Schuster is with the Institute of Electrical Drive Systems, Technical University Munich, Munich 80333, Germany (e-mail: hans.schuster@tum.de).

Digital Object Identifier 10.1109/TAC.2009.2013013

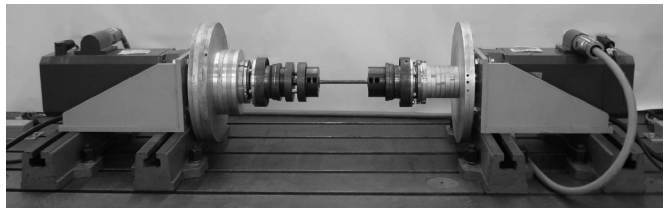

Fig. 1 Two mass system (test rig); elastic shaft: 120 mm long, 9 mm diameter, overall length appr. 1.5 m.

II. The Model

Generally, a nonlinear two mass system with friction is modelled, see [3, Sec. 2], as

$$\left.\begin{aligned}\dot{x}(t) &= Ax(t)+b_N\left[g\omega_\ell(t)+(\mathbf{N}\omega_\ell)(t)\right]+b\left[u(t)+\hat{d}(t)\right]\\ y(t) &= cx(t)\end{aligned}\right\} \tag{1}$$

with $c=(c_1,c_2,c_3)\in\mathbb{R}^{1\times 3}$ and

$$A=\begin{bmatrix}\frac{-d}{J_\ell} & \frac{k}{J_\ell} & \frac{d}{J_\ell}\\ -1 & 0 & 1\\ \frac{d}{J_d} & \frac{-k}{J_d} & \frac{-d}{J_d}\end{bmatrix},\quad b_N=\begin{pmatrix}\frac{-1}{J_\ell}\\ 0\\ 0\end{pmatrix},\quad b=\begin{pmatrix}0\\ 0\\ \frac{1}{J_d}\end{pmatrix}$$

and constants: $J_d, J_\ell > 0$ moments of inertia (drive-mass and load-mass), $d,k>0$ damping and stiffness coefficient (elastic shaft), $g\geq 0$ coefficient of the viscous friction. The state variables $x(t)=(\omega_\ell(t),\alpha(t),\omega_d(t))^T$ denote the speed of the load, the angle of twist between drive and load and the speed of the drive at time t, resp., and $\hat{d}\in L^\infty(\mathbb{R};\mathbb{R})$ denotes an arbitrary bounded input disturbance. Since a power converter is not modeled in A in (1), this is incorporated by $\hat{d}$. To include nonlinear effects like friction the nonlinear causal operator $\mathbf{N}: C([-h,\infty);\mathbb{R})\to L^\infty([0,\infty);\mathbb{R})$, is used where $h\geq 0$ quantifies its "memory". The operator is assumed to satisfy the *global boundedness* condition

$$\sup\left\{|(\mathbf{N}\zeta)(t)|\,|\,t\geq 0,\zeta\in C([-h,\infty);\mathbb{R})\right\}<\infty \tag{2}$$

and belongs to the following class $\mathcal{T}$:

i) $T: C([-h,\infty);\mathbb{R})\to L^\infty_{\mathrm{loc}}(\mathbb{R}_{\geq 0};\mathbb{R})$, for some $h\geq 0$;

ii) *bounded-input, bounded-output*: $\forall\delta>0\exists\Delta>0\forall\zeta\in C([-h,\infty);\mathbb{R})$: $[\sup_{t\in[-h,\infty)}|\zeta(t)|\leq\delta\Rightarrow|(T\zeta)(s)|\leq\Delta$ a.a. $s\geq 0]$;

iii) For all $t\geq 0$, the following hold: *causality*: $\forall\zeta,\psi\in C([-h,\infty);\mathbb{R})$ with $\zeta(\cdot)\equiv\psi(\cdot)$ on $[-h,t]$: $(T\zeta)(s)=(T\psi)(s)$ a. a. $s\in[0,t]$; *locally Lipschitz*: $\forall\beta\in C([-h,t];\mathbb{R})\exists\tau,\delta,c>0\forall\zeta,\psi\in C([-h,\infty);\mathbb{R})$ with $\zeta|_{[-h,t]}=\beta=\psi|_{[-h,t]}$ and $\zeta(s),\psi(s)\in[\beta(t)-\delta,\beta(t)+\delta]\forall s\in[t,t+\tau]$: $\mathrm{ess}-\sup_{s\in[t,t+\tau]}|(T\zeta)(s)-(T\psi)(s)|\leq c\cdot\sup_{s\in[t,t+\tau]}|\zeta(s)-\psi(s)|$.

If $\mathbf{N}$ satisfies (2), then (i) and (ii) are trivially satisfied. The wide range of the operator class $\boldsymbol{\mathcal{T}}$ encompasses–even if restricted by (2)—phenomena such as nonlinear friction, relay hysteresis, backlash hysteresis, elastic-plastic hysteresis, Preisach or Prantl hysteresis, see [8] and [4]. In view of (2), $\mathbf{N}$ cannot model viscous friction $\omega_\ell(\cdot)\mapsto g\omega_\ell(\cdot)$. To overcome this, the friction characteristic is split into a sum of a bounded nonlinear operator $(\mathbf{N}\omega_\ell)(\cdot)$ (modelling Coulomb-friction, Stribeck-effect, etc.) and an unbounded term $g\omega_\ell(\cdot)$. The latter is added to the linear dynamics. ◇

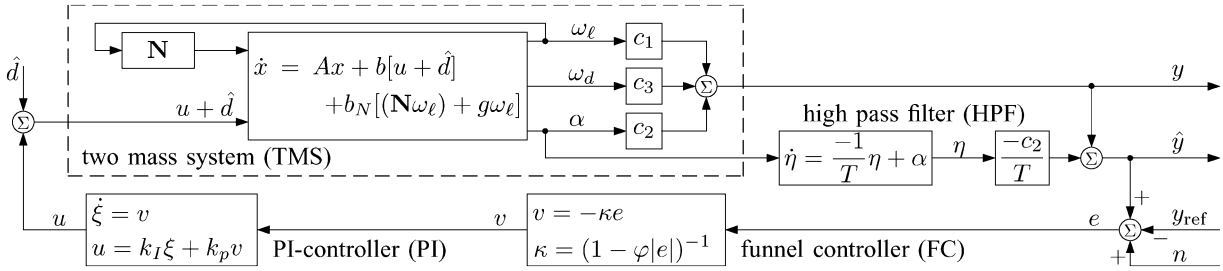

Fig. 2 Block diagram for the overall control loop.

Remark 2.1: Since (1) is a functional differential equation, the appropriate initial data are

$$x|_{[-h,0]} = \left(\omega_\ell^0(\cdot), \alpha^0, \omega_d^0\right)^T \in C\left([-h,0];\mathbb{R}\right) \times \mathbb{R} \times \mathbb{R}. \tag{3}$$

By a solution $x : [-h,\omega) \to \mathbb{R}^3$ of the initial value problem (1), (3) with locally integrable input $u : [0,\infty) \to \mathbb{R}$, we mean that $x \in C([-h,\omega);\mathbb{R}^3)$, with $0 < \omega \leq \infty$, $x|_{[-h,0]} = x^0$, such that $x|_{[0,\omega)}$ is absolutely continuous and satisfies (1) for almost all $t \in [0,\omega)$.

It is shown in [6, Th. 4.2] that the functional initial value problem (1), (3) has, for any initial data (3) and feedback as depicted in Fig. 2 and specified in Theorem 4.1, a unique solution which can be maximally extended on $[-h,\omega)$, $0 < \omega \leq \infty$, and if this solution is bounded, then $\omega = \infty$. ◇

Remark 2.2: If the output vector $c = (c_1, c_2, c_3) \in \mathbb{R}^{1\times 3}$ satisfies $c_3 \neq 0$, then the coordinate transformation $y(t) := c_1\omega_\ell(t) + c_2\alpha(t) + c_3\omega_d(t)$ converts (1) into the equivalent system in *Byrnes–Isidori normal form*

$$\begin{aligned}\frac{\mathrm{d}}{\mathrm{d}t}y(t) &= a_1 y(t) + a_2\begin{pmatrix}\omega_\ell(t)\\ \alpha(t)\end{pmatrix} - \frac{c_1}{J_\ell}(\mathbf{N}\omega_\ell)(t)\\ &\quad + \frac{c_3}{J_d}\hat{d}(t) + \frac{c_3}{J_d}u(t) \qquad (4a)\\ \frac{\mathrm{d}}{\mathrm{d}t}\begin{pmatrix}\omega_\ell(t)\\ \alpha(t)\end{pmatrix} &= \Lambda\begin{pmatrix}\omega_\ell(t)\\ \alpha(t)\end{pmatrix} + \begin{pmatrix}\frac{d}{c_3 J_\ell}\\ \frac{1}{c_3}\end{pmatrix}y(t)\\ &\quad - \begin{pmatrix}\frac{1}{J_\ell}\\ 0\end{pmatrix}(\mathbf{N}\omega_\ell)(t) \qquad (4b)\end{aligned}$$

where $a_1 = [(c_1 - c_3 J_\ell/J_d)d + c_2 J_\ell]/[c_3 J_\ell]$

$$a_2 = \begin{pmatrix} -\frac{d(c_1c_3+c_1^2)}{c_3 J_\ell} + \frac{d(c_1+c_3)}{J_d} - c_2 - \frac{c_1c_2}{c_3} - \frac{c_1 g}{J_\ell} \\ \frac{c_1c_3k - c_1c_2d - 2c_2^2 J_\ell}{c_3 J_\ell} + \frac{c_2 d - c_3 k}{J_d} + \frac{c_2^2}{c_3}\end{pmatrix}^T$$

$$\Lambda = \begin{bmatrix} -\frac{d(c_1+c_3)+c_3 g}{c_3 J_\ell} & \frac{c_3 k - c_2 d}{c_3 J_\ell} \\ \frac{-(c_1+c_3)}{c_3} & -\frac{c_2}{c_3}\end{bmatrix}.$$

Note that (4) is a functional differential equation, in particular it may be a delay differential equation. ◇

Remark 2.3: If the output vector c in (1) is considered as a design parameter, then the following relationships are essential for the stability properties of the model

$$c_3 > 0, \qquad c_2 \geq 0, \qquad c_1 > -c_3. \tag{5}$$

A straightforward calculation gives: (i) (5) implies $\mathrm{spec}(\Lambda) \subset \mathbb{C}_-$, hence the two mass system with $\mathbf{N} \equiv 0$ is minimum-phase; (ii) if $\mathrm{spec}(\Lambda) \subset \mathbb{C}_-$, then an application of the Variation-of-Constants formula to (4b) and exploiting (2) yields that (4b) is $L^\infty(\mathbb{R}_{\geq 0};\mathbb{R})$-input y to $L^\infty(\mathbb{R}_{\geq 0};\mathbb{R})$-state (ω_ℓ, α) stable; (iii) if $\mathrm{spec}(\Lambda) \subset \bar{\mathbb{C}}_-$, then (4) has bounded zero dynamics or, if $\mathbf{N} \equiv 0$, it has asymptotically stable zero dynamics. Bounded (asymptotically stable) zero dynamics means that all possible dynamics with $y \equiv 0$ are bounded or asymptotically stable, resp.; for further details see [4, Sect. 2.3] and the references therein. ◇

Invoking (4) and assuming (5), it is easy to show that the system (1) is practically high-gain stabilizable in the sense that for any $\varepsilon > 0$ there exists $\kappa > 0$ sufficiently large so that $u(t) = -\kappa y(t)$ applied to (1) yields $\limsup_{t\to\infty} |y(t)| \leq \varepsilon$.

Proposition 2.4: Suppose (5) holds. Then (1) with initial data (3) may be written, for some $\mathbf{T} \in \mathcal{T}$ and $p \in L^\infty(\mathbb{R}_{\geq 0};\mathbb{R})$, as

$$\left.\begin{aligned}\tfrac{\mathrm{d}}{\mathrm{d}t}y(t) &= (\mathbf{T}y)(t) + p(t) + \tfrac{c_3}{J_d}u(t)\\ y|_{[-h,0]} &= c\left(\omega_\ell^0(\cdot), \alpha^0, \omega_d^0\right)^T.\end{aligned}\right\} \tag{6}$$

Proof: Consider (4) and set

$$\begin{aligned}&\mathbf{T_1} : L^\infty_{\mathrm{loc}}(\mathbb{R}_{\geq 0};\mathbb{R}^2) \to L^\infty_{\mathrm{loc}}(\mathbb{R}_{\geq 0};\mathbb{R}^2)\\ &\quad \zeta(\cdot) \mapsto \int_0^{\cdot} e^{\Lambda(\cdot - s)}\zeta(s)\mathrm{d}s\\ &p(\cdot) := a_2 e^{\Lambda\cdot}\begin{pmatrix}\omega_\ell^0(0)\\ \alpha^0\end{pmatrix} + a_2\left(\mathbf{T_1}\begin{pmatrix}\frac{-1}{J_\ell}\\ 0\end{pmatrix}(\mathbf{N}\omega_\ell)\right)(\cdot)\\ &\qquad - \frac{c_1}{J_\ell}(\mathbf{N}\omega_\ell)(\cdot) + \frac{c_3}{J_d}\hat{d}(\cdot)\\ &(\mathbf{T}y)(\cdot) := a_1 y(\cdot) + a_2\left(\mathbf{T_1}\begin{pmatrix}\frac{d}{c_3 J_\ell}\\ \frac{1}{c_3}\end{pmatrix}y\right)(\cdot).\end{aligned}$$

Invoking (2), Remark 2.3 and $\hat{d} \in L^\infty(\mathbb{R};\mathbb{R})$, it follows from [5, Subsection 4.1] that $\mathbf{T_1} \in \mathcal{T}$, $p \in L^\infty(\mathbb{R}_{\geq 0};\mathbb{R})$, and also $\mathbf{T} \in \mathcal{T}$. Hence we may apply variation of constants to (4b) and substituting this into (4a) yields, with the above notation, (6). □

III. Funnel Control

The *control objective* is to design a feedback strategy which ensures, with reference to Fig. 2, for every reference signal $y_{\mathrm{ref}} \in W^{1,\infty}(\mathbb{R}_{\geq 0};\mathbb{R})$, i.e. the space of bounded, locally absolutely continuous signals with essentially bounded derivative, and every disturbance signal $\hat{d} \in L^\infty(\mathbb{R};\mathbb{R})$: (i) the output error $e = \hat{y} - y_{\mathrm{ref}}$ evolves within the funnel; (ii) the output error $e(t)$ is, for prespecified time $\tau > 0$ onwards, smaller that a prespecified tracking accuracy $\lambda_\tau > 0$; (iii) all signals in the closed-loop system are bounded; (iv) oscillations in the elastic shaft are damped; (v) any disturbance $\hat{d} \in L^\infty(\mathbb{R};\mathbb{R})$ is rejected.

The control objectives are captured by the concept of funnel control as introduced by [5]: A prespecified *performance funnel*

$$\mathcal{F}_\varphi := \{(t,e) \in \mathbb{R}_{\geq 0} \times \mathbb{R} | \varphi(t)|e| < 1\}$$

is associated with a function φ (the reciprocal of which determines the funnel boundary) of the class

$$\Phi_\lambda := \left\{\varphi \in W^{1,\infty}(\mathbb{R}_{\geq 0}, \mathbb{R}_{\geq 0}) | \varphi(0) = 0, \right.$$
$$\left. \varphi(s) > 0\ \forall s > 0, \liminf_{s\to\infty} \varphi(s) > \lambda^{-1}\right\}$$

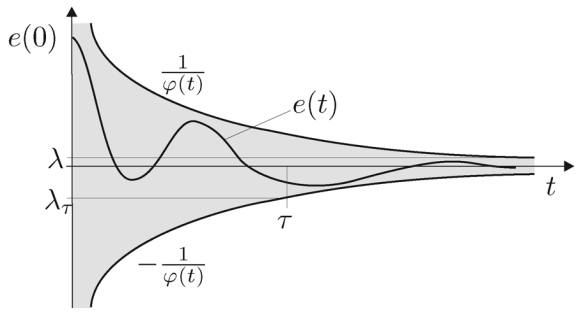

Fig. 3 Prescribed performance funnel $\mathcal{F}_\varphi$.

where $\lambda > 0$ describes the "ultimate width" of the funnel, see Fig. 3.

The control objectives (i) and (ii) are captured by the funnel controller (12). For example, if φ is chosen as the function $t \mapsto \min\{t/\tau, 1\}/\lambda_\tau$, then evolution within the funnel ensures that the prescribed tracking accuracy $\lambda_\tau > 0$ is achieved within the prescribed time $\tau > 0$. Objective (iv) is taking care of by introducing the high pass filter (7). The objective (iii) is addressed by the conjunction of all three controllers.

Before introducing the funnel controller in (12), we introduce the high pass filter and the PI-controller. Conjunct, with reference to Fig. 2, the high-pass filter (HPF)

$$\dot\eta(t) = -\frac{1}{T}\eta(t) + \alpha(t), \qquad \eta(0) = 0 \tag{7}$$

for a design parameter $T > 0$ with the output y by defining the new output

$$\hat y(t) = y(t) - \frac{c_2}{T}\eta(t). \tag{8}$$

The high-pass filter does, loosely spoken, detect in the new output whether the angle of twist $\alpha(\cdot)$ oscillates or not. If $\alpha(\cdot) \approx \text{const.}$, then $\hat y(\cdot) \approx y(\cdot) - (c_2/T)T\ \text{const.} = c_1\omega_\ell(\cdot) + c_3\omega_d(\cdot)$, and so $\alpha(\cdot)$ pays no contribution in $\hat y(\cdot)$. If $\alpha(\cdot)$ contains oscillations as high frequencies, they pass the filter with nearly no attenuation, and since the input of the filter passes the feed-through path without any delay, every change of the input is visible in the output $\hat y$ immediately.

It has been observed in [9] that the application of the funnel controller (12) alone exhibits a nonzero error in the steady state. To overcome this drawback we introduce—see also Fig. 2—a PI-controller as a pre-compensator to (1):

$$u(t) = k_I\xi(t) + k_P v(t), \xi(0) = 0, \quad \frac{\mathrm{d}}{\mathrm{d}t}\xi(t) = v(t) \tag{9}$$

with design parameters $k_I, k_P > 0$.

It is easy to see, that the control error vanishes, if a steady state is attained, i.e. $\lim_{t\to\infty}(\mathrm{d}/\mathrm{d}t)\xi(t) = 0$. From (9) it follows that a steady state for ξ is equivalent to $\lim_{t\to\infty} v(t) = 0$, and thus a proportional error feedback $v(t) = -\kappa(t)e(t)$ yields $\lim_{t\to\infty} e(t) = 0$, provided that $\limsup_{t\to\infty}\kappa(t) > 0$.

Proposition 3.1 [(1) & (HPF-PI)]: Suppose (5) holds. Then the nominal system (1) with initial data (3) in conjunction with (i) the high-pass filter (7), (8) for $T > 0$ and/or (ii) the PI-controller (9) for $k_I, k_P > 0$, may be written, for some $\hat{\mathbf{T}} \in \mathcal{T}$, $\hat p \in L^\infty(\mathbb{R}_{\geq 0};\mathbb{R})$, $\hat c \in \mathbb{R}\setminus\{0\}$, as

$$\left.\begin{aligned} \tfrac{\mathrm{d}}{\mathrm{d}t}\hat y(t) &= (\hat{\mathbf{T}}\hat y)(t) + \hat p(t) + \hat c u(t)\\ \hat y|_{[-h,0]} &= c\left(\omega_\ell^0(\cdot), \alpha^0, \omega_d^0\right)^T. \end{aligned}\right\} \tag{10}$$

Proof: First, consider the augmented input-output system (1), (7), (8) with (3), which may be written, by introducing $\hat y(t) = c_1\omega_\ell(t) + c_2\alpha(t) + c_3\omega_d(t) - (c_2/T)\eta(t)$, in Byrnes-Isidori normal form

$$\left.\begin{aligned} \tfrac{\mathrm{d}}{\mathrm{d}t}\hat y(t) &= \hat a_1\hat y(t) + \hat a_2\,(\omega_\ell(t)\quad \alpha(t)\quad \eta(t))^T\\ &\quad -\tfrac{c_1}{J_\ell}(\mathbf{N}\omega_\ell)(t) + \tfrac{c_3}{J_d}\hat d(t) + \tfrac{c_3}{J_d}u(t),\\ \tfrac{\mathrm{d}}{\mathrm{d}t}\begin{pmatrix}\omega_\ell(t)\\ \alpha(t)\\ \eta(t)\end{pmatrix} &= \hat\Lambda\begin{pmatrix}\omega_\ell(t)\\ \alpha(t)\\ \eta(t)\end{pmatrix} - \begin{pmatrix}\frac{1}{J_\ell}\\ 0\\ 0\end{pmatrix}(\mathbf{N}\omega_\ell)(t)\\ &\quad + \begin{pmatrix}\frac{d}{c_3 J_\ell} & \frac{1}{c_3} & 0\end{pmatrix}^T\hat y(t), \end{aligned}\right\} \tag{11}$$

where $\hat a_1 \in \mathbb{R}$, $\hat a_2 \in \mathbb{R}^{1\times 3}$ are appropriate and

$$\hat\Lambda = \begin{bmatrix} -\frac{d(c_1+c_3)+c_3 g}{c_3 J_\ell} & \frac{c_3 k - c_2 d}{c_3 J_\ell} & \frac{c_2 d}{c_3 T J_\ell}\\ \frac{-(c_1+c_3)}{c_3} & -\frac{c_2}{c_3} & \frac{c_2}{c_3 T}\\ 0 & 1 & \frac{-1}{T}\end{bmatrix}.$$

A simple calculation shows that $\operatorname{spec}\hat\Lambda \subset \mathbb{C}_-$. To show that (11) can be written as (10) is analogous to the proof of Proposition 2.4.

For brevity, we omit the proof that (1) in conjunction with the PI-controller (9) can be written as (10); the proof is a simplification of the following.

It remains to consider the conjunction of the nominal system (1) with initial data (3) in conjunction with the high-pass filter (7), (8) and the PI-controller (9); this conjunction is, by writing $\hat y(t) = c_1\omega_\ell(t) + c_2\alpha(t) + c_3\omega_d(t) - (c_2/T)\eta(t)$ and $\zeta(t) = \hat y(t) - c_3(k_P/J_d)\xi(t)$ equivalent to the Byrnes-Isidori normal form

$$\left.\begin{aligned} \tfrac{\mathrm{d}}{\mathrm{d}t}\hat y(t) &= \tilde a_1\hat y(t) + \tilde a_2\,(\omega_\ell(t)\ \alpha(t)\ \eta(t)\ \zeta(t))^T\\ &\quad -\tfrac{c_1}{J_\ell}(\mathbf{N}\omega_\ell)(t) + \tfrac{c_3}{J_d}\left[k_P v(t) + \hat d(t)\right],\\ \tfrac{\mathrm{d}}{\mathrm{d}t}\begin{pmatrix}\omega_\ell(t)\\ \alpha(t)\\ \eta(t)\\ \zeta(t)\end{pmatrix} &= \tilde\Lambda\begin{pmatrix}\omega_\ell(t)\\ \alpha(t)\\ \eta(t)\\ \zeta(t)\end{pmatrix} - \begin{pmatrix}1/J_\ell\\ 0\\ 0\\ c_1/J_\ell\end{pmatrix}(\mathbf{N}\omega_\ell)(t)\\ &\quad + \tilde a_4\hat y(t) + (0\ 0\ 0\ c_3/J_d)^T\hat d(t), \end{aligned}\right\}$$

where $\tilde a_1 \in \mathbb{R}$, $\tilde a_2, \tilde a_4^T \in \mathbb{R}^{1\times 4}$ are appropriate and

$$\tilde\Lambda = \begin{bmatrix} \frac{d(c_1+c_3)+c_3 g}{-c_3 J_\ell} & \frac{c_3 k - c_2 d}{c_3 J_\ell} & \frac{c_2 d}{c_3 T J_\ell} & 0\\ \frac{c_1+c_3}{-c_3} & \frac{-c_2}{c_3} & \frac{c_2}{c_3 T} & 0\\ 0 & 1 & \frac{-1}{T} & 0\\ * & * & * & \frac{-k_I}{k_P}\end{bmatrix}.$$

Since $\operatorname{spec}\tilde\Lambda = \operatorname{spec}\hat\Lambda \cup \{-k_I/k_P\}$, the remainder of the proof is completely analogous to the proof of Proposition 2.4. □

Finally, we introduce the funnel controller in conjunction with the high-pass filter (7), (8) and/or the PI-controller (9): set, for $\lambda > 0$ and $\varphi \in \Phi_\lambda$

$$v(t) = -\kappa(t)e(t), \qquad \kappa(t) = \frac{1}{1 - \varphi(t)\,|e(t)|}. \tag{12}$$

IV. Main Result

The control objectives (i)–(v) of Section III are now addressed by the conjunction of the high pass filter (7), PI-controller (9) and funnel controller (12). Note the simplicity of all three controllers and that they do depend only on structural system assumptions.

Theorem 4.1: Suppose (5) holds. Let a funnel $\mathcal{F}_\varphi$ be determined by $\varphi \in \Phi_\lambda$ for $\lambda > 0$. Then the application of each of the following controllers

(FC)	funnel controller (12), $e(t) = y(t) - y_{\mathrm{ref}}(t)$, $v(t) = u(t)$;
(HPF-FC)	high-pass filter (7), funnel controller (12), $e(t) = \hat{y}(t) - y_{\mathrm{ref}}(t)$, $v(t) = u(t)$;
(PI-FC)	funnel controller (12), $e(t) = y(t) - y_{\mathrm{ref}}(t)$, PI-controller (9), $k_I, k_P > 0$;
(HPF-PI-FC)	high-pass filter (7), funnel controller (12), $e(t) = \hat{y}(t) - y_{\mathrm{ref}}(t)$, PI-controller (9), $k_I, k_P > 0$;

in conjunction with any nominal system (1) yields, for arbitrary initial data $x|_{[-h,0]} = (\omega_\ell^0(\cdot), \alpha^0, \omega_d^0)^T \in C([-h,0];\mathbb{R}) \times \mathbb{R} \times \mathbb{R}$ and arbitrary reference signal $y_{\mathrm{ref}} \in W^{1,\infty}(\mathbb{R}_{\geq 0};\mathbb{R})$, (i) a closed-loop initial value problem which has a solution, (ii) every solution has a maximal extension on $[0,\infty)$, (iii) every solution component is bounded on $[0,\infty)$, (iv) there exists $\varepsilon \in (0,1)$ such that, for all $t > 0$, $|e(t)| \leq (1-\varepsilon)\varphi(t)^{-1}$, (v) if the PI-controller is invoked, then, for all $t \geq 0$, $|e(t)| < |\dot{\xi}(t)|$. ◇

Proof: We consider the four different control schemes.

(FC): By Proposition 2.4, the input-output system (1) may be written as (6) and the latter satisfies all assumptions required in [5, Th. 7] so that the application of the funnel controller (12), $e(t) = y(t) - y_{\mathrm{ref}}(t)$ ensures all assertions claimed in the theorem.

To see (HPF-FC), (PI-FC) and (HPF-PI-FC), use Proposition 3.1 and argue as in (FC) above.

Finally, assertion (ii), in case of (PI-FC) or (HPF-PI-FC), follows from $\dot{\xi}(t) = -\kappa(t)e(t)$ and the fact that $\kappa(t) > 1$. □

Corollary 4.2 [Tracking of the Load]: Suppose (5) holds. Let $\omega_{\mathrm{ref}} \in W^{1,\infty}(I;\mathbb{R})$ be a prespecified reference signal for the speed of the load. Let a funnel $\mathcal{F}_\varphi$ be determined by $\varphi \in \Phi_\lambda$ and $\lambda > 0$. Then the application of the four controllers investigated in Theorem 4.1 for

$$y_{\mathrm{ref}}(\cdot) := (c_1 + c_3)\omega_{\mathrm{ref}}(\cdot) \tag{13}$$

to any system (1) yields, for arbitrary initial data $x|_{[-h,0]} = (\omega_\ell^0(\cdot), \alpha^0, \omega_d^0)^T \in C([-h,0];\mathbb{R}) \times \mathbb{R} \times \mathbb{R}$, a closed-loop initial value problem with properties described in Theorem 4.1 and moreover the difference between the load and the load reference signal satisfies, for all $t \geq 0$,

(FC)	$\omega_\ell(t) - \omega_{\mathrm{ref}}(t) = (1/(c_1+c_3))[e(t) - c_2\alpha(t) - c_3\dot{\alpha}(t)]$;
(HPF-FC)	$\omega_\ell(t) - \omega_{\mathrm{ref}}(t) = (1/(c_1+c_3))[e(t) - c_2\alpha(t) - c_3\dot{\alpha}(t) + (c_2/T)\eta(t)]$;
(PI-FC)	$\omega_\ell(t) - \omega_{\mathrm{ref}}(t) = (1/(c_1+c_3))[-\kappa(t)^{-1}\dot{\xi}(t) - c_2\alpha(t) - c_3\dot{\alpha}(t)]$;
(HPF-PI-FC)	$\omega_\ell(t) - \omega_{\mathrm{ref}}(t) = (1/(c_1+c_3))[-\kappa(t)^{-1}\dot{\xi}(t) - c_2\alpha(t) - c_3\dot{\alpha}(t) + (c_2/T)\eta(t)]$.

Proof: We consider the four different control schemes as in Theorem 4.1. Then (1) and (13) give $y - y_{\mathrm{ref}} = (c_1+c_3)(\omega_\ell - \omega_{\mathrm{ref}}) + c_2\alpha + c_3(\omega_d - \omega_\ell)$ and, in view of $\dot{\alpha} = \omega_d - \omega_\ell$, the statement for (FC) follows. Next consider (HPF-FC) which gives $\hat{y} - y_{\mathrm{ref}} = (c_1+c_3)(\omega_\ell - \omega_{\mathrm{ref}}) + c_2\alpha + c_3(\omega_d - \omega_\ell) - (c_2/T)\eta$ and, in view of $\dot{\alpha} = \omega_d - \omega_\ell$ and (7), the statement follows. The statement (PI-FC) follows from the statement (FC) by substituting $e = -\kappa^{-1}\dot{\xi}$, which is a consequence of the first equation in (9) in conjunction with $v = -\kappa e$, into the statement (FC). Finally, to show the statement (HPF-PI-FC), substitute $e = -\kappa^{-1}\dot{\xi}$ into the statement (HPF-FC). This completes the proof of the corollary. □

Corollary 4.2 elucidates how the different controllers effect $\omega_\ell - \omega_{\mathrm{ref}}$. Although $e(t)$ may be forced by the funnel controller to be arbitrarily small, the deviation $\omega_\ell(t) - \omega_{\mathrm{ref}}(t)$ is not necessarily small in the case (FC). To obtain $\omega_\ell(t) - \omega_{\mathrm{ref}}(t) \equiv 0$, the state trajectory $\alpha(\cdot)$ must satisfy the differential equation

$$\dot{\alpha}(t) = -\frac{c_2}{c_3}\alpha(t) + \frac{1}{c_3}e(t)$$

which, in general contradicts the dynamics of the plant. Even if $c_2 = 0$, a perfect control performance is not attainable since no active damping is provided. Vibrations vanish by using $c_2 \neq 0$, but in the steady state, where $\alpha(t) \neq 0$ is proportional to the applied load torque and $\dot{\alpha}(t) = 0$, a deviation is caused. For this reason, we cannot expect that $\omega_\ell(t)$ converges to a desired setpoint $\omega_{\mathrm{ref}}(\cdot) = \mathrm{const}$.

(HPF) is introduced to cancel $c_2\alpha(t)$ in the steady state by adding the term $(c_2/T)\eta(t)$. From (7) and $\dot{\eta}(t) = 0$ it follows that $(c_2/T)\eta(t) - c_2\alpha(t) = 0$. Since in the steady state $\dot{\alpha}(t) = 0$ holds true, the deviation $\omega_\ell(t) - \omega_{\mathrm{ref}}(t)$ is proportional to $e(t)$. If additionally (PI) is used, then the control error $e(t)$ gets substituted by $-\kappa(t)^{-1}\dot{\xi}(t)$. The benefit is, that a large funnel is applicable (what permits the toleration of measurement noise) without deterioration of the steady state deviation. Since $\dot{\xi} = 0$ if the control loop converges to the steady state, no deviation $\omega_\ell - \omega_{\mathrm{ref}}$ results from e.

V. Experimental Results

We consider the two mass system depicted in Fig. 1. It is located in the laboratory of the Institute of Electrical Drive Systems, Technical University of Munich, and serves for investigating the behaviour of drives with elastic coupling between motor and mechanics. The four controllers of this technical note have been tested at it.

The approximate plant parameters in (1) are, see [1]: $J_d = 0.166$ [kg m^2], $J_\ell = 0.333$ [kg m^2], $d = 0.025$ [Nm s/rad], $k = 410$ [Nm/rad], $g = 0.0018$ [Nm s/rad]. Note that they are not used at all for the control.

The actual plant is controlled by the four control schemes (FC), (HPF-FC), (PI-FC) and (HPF-PI-FC) considered in Theorem 4.1 and Corollary 4.2. For all cases, the funnel $\mathcal{F}_\varphi \in \Phi_\lambda$ is defined by $t \mapsto \varphi(t) = (150 \cdot \exp\{-2t^2\} + 80)^{-1}$. Note that $\lambda = 80$ but $\varphi \notin \Phi_\lambda$ since $\varphi(0) = 1/230$. However, Theorem 4.1 and Corollary 4.2 remain valid as long as $|e(0)| < \varphi(0)^{-1}$. The reference signal $t \mapsto \omega_{\mathrm{ref}}(t) = 30 \cdot (1 - \exp\{-t/0.3\})$ [rad/sec] is depicted by a dotted line in Fig. 4. To examine the rejection of disturbances caused by the driven mechanics, a constant load $M_\ell = 10$ [Nm] is injected at time $t = 10$ [sec]. An input disturbance $\hat{d}$ is not applied externally, but is present due to the non-ideal behaviour of the power converter.

The simulation study in [9] demonstrates the influence of the weighting factor c_2 if funnel control (FC) is used without any extension. The friction or a load torque causes a deviation in the steady state; this is typical for proportional controllers. The deviation stays small, if c_2 is small. However, during the transient period large oscillations occur. These oscillations are excited for example if the load changes abruptly or by periodic action of the friction force and cannot be damped by the controller actively as long as the angle of twist is not included in the feedback signal.

The damping improves considerably if c_2 is enlarged. Then the angle of twist α plays a significant rôle in the feedback signal which yields active damping. However, Corollary 4.2 (FC) shows that the deviation $\omega_\ell(t) - \omega_{\mathrm{ref}}(t)$ increases due to the term $c_2\alpha(t)$, wherein $\alpha(t) = [M_\ell + g\omega_\ell(t) + (\mathbf{N}\omega_\ell)(t)]/k$ depends on the unknown load torque M_ℓ, the unknown parameters g and $\mathbf{N}$ of the friction characteristic and on the unknown stiffness k.

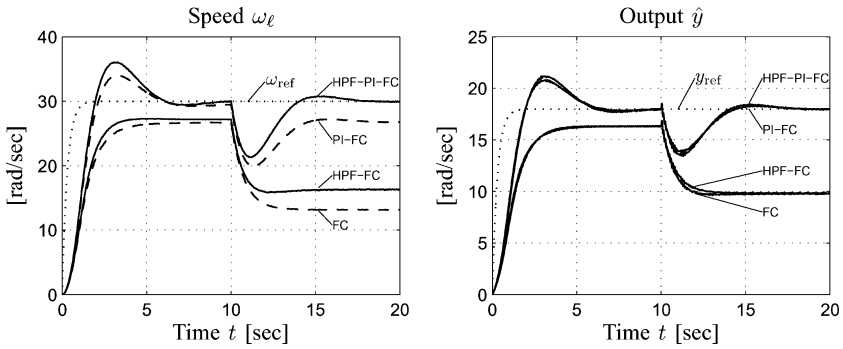

Fig. 4 Experimental results. Left hand side: speed ω_ℓ under funnel control with different extensions; Right hand side: output $\hat{y}$.

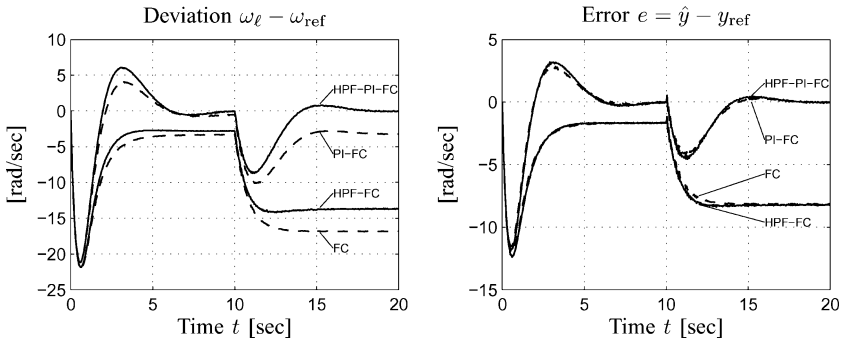

Fig. 5 Experimental results. Left hand side: deviation $\omega_\ell - \omega_{\rm ref}$ under funnel control with different extensions. Right hand side: control error $e = \hat{y} - y_{\rm ref}$.

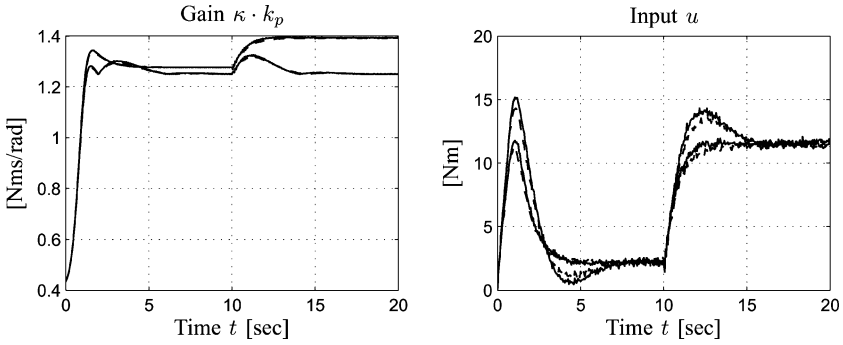

Fig. 6 Experimental results. Left hand side: gain $\kappa \cdot k_p$ under funnel control with different extensions. Right hand side: input u.

Theses observations underpin the necessity for funnel control and it is confirmed by our experiments, to choose a large value c_2 and to compensate its effects by a PI-controller and a high pass filter. Consequently, a state feedback with a large c_2 is used for the experiments where the design parameter vector c is set to $c = (0.1, 80, 0.5)$.

The different effects of the PI and HPF extensions are depicted in Figs. 4–6. On the left hand side of Fig. 4 the speed $\omega_\ell = (1, 0, 0)x$ is depicted together with the desired speed trajectory $\omega_{\rm ref}(\cdot)$.

Due to the choice $c_2 = 80$, all oscillations in the shaft are suppressed adequately. The funnel controller (FC) however is not able to produce steady state accuracy. The friction torque reduces the speed ω_ℓ to approximately 26.7 [rad/s]. With the additional load (10 [Nm]) the speed slows down to 13.2 [rad/s], which corresponds to a control error of about 56%.

To improve the accuracy, (PI-FC) is employed. Then the output $\hat{y}$ is forced to the reference value $y_{\rm ref}$ and the remaining error e is reduced to zero asymptotically, even if load is present. Although the controller accomplishes its task ($e \to 0$), the speed ω_ℓ does not converge to the desired value $\omega_{\rm ref}$. Corollary 4.2 shows that the angle of twist $\alpha \neq 0$ (caused by friction or load) leads to an additive term and is therefore the reason why the PI-extension is not sufficient.

The purpose of the high pass filter is to eliminate the additive term $c_2\alpha$ in (HPF-FC) without erasing important information from the signal $\hat{y}$. Moreover, oscillations are weighted by $c_2 = 80$ and are included in $\hat{y}$. Therefore, the desired damping is maintained. In the steady state however constant $\alpha \neq 0$ is suppressed by the (HPF). Since $c_2\alpha$ is not present, the deviation is reduced by this value.

The combination of the funnel controller (FC) with $c_2 \neq 0$ together with (HPF) gives, in the steady state, the same value for ω_ℓ as a funnel controller with $c_2 = 0$ does. However, compared to (FC) with $c_2 = 0$ the (HPF-FC) reveals the advantage of better damping.

These measurement results and theoretical investigations suggest that the extension of funnel control with either (PI) or (HPF) attains not a satisfying improvement. Hence (HPF-PI-FC) as depicted in Fig. 2 is finally applied and the results are depicted in Fig. 4. The integrating contribution in the control action forces $\dot{\xi}$ to vanish, which is equivalent to $e \to 0$ (see Fig. 5). Hence the controlled variable $\hat{y}$ converges to the reference value $y_{\rm ref}$, even if load is applied. Because

(HPF) eliminates the effect of α asymptotically in the feedback signal by cancelling the term αc_2, no deviation remains. Thus $e \to 0$ causes ω_ℓ to converge to the desired value $\omega_{\rm ref}$.

REFERENCES

[1] B. T. Angerer, C. Hintz, and D. Schröder, "Online identification of a nonlinear mechatronic system," *Control Eng. Pract.*, vol. 12, pp. 1465–1478, 2004.

[2] H. Schuster, D. Schröder, and C. Westermaier, "Mechatronic—Advanced computational intelligence," in *Proc. Int. Conf. Power Electron. Drive Syst., PEDS*, Bangkok, Thailand, 2007, pp. 994–1001.

[3] D. Schröder, *Intelligent Observer and Control Design for Nonlinear Systems*. Berlin, Germany: Springer-Verlag, 2000.

[4] A. Ilchmann, E. P. Ryan, and C. J. Sangwin, "Systems of controlled functional differential equations and adaptive tracking," *SIAM J. Control Optim.*, vol. 40, pp. 1746–1764, 2002.

[5] A. Ilchmann, E. P. Ryan, and C. J. Sangwin, "Tracking with prescribed transient behaviour," *ESAIM Control, Opt. Calculus Var.*, vol. 7, pp. 471–493, 2002.

[6] A. Ilchmann, E. P. Ryan, and P. Townsend, "Tracking with prescribed transient behaviour for nonlinear systems of known relative degree," *SIAM J. Control Optim.*, vol. 46, pp. 210–230, 2007.

[7] A. Ilchmann and E. P. Ryan, "Adaptive and non-adaptive control without identification: A survey," *GAMM Mitt.*, vol. 31, no. 1, pp. 115–125, 2008.

[8] H. Logemann and A. D. Mawby, "Low-gain integral control of infinite dimensional regular linear systems subject to input hysteresis," in *Advances in Mathematical Systems Theory*, F. Colonius, U. Helmke, D. Prätzel-Wolters, and F. Wirth, Eds. Boston, MA: Birkhäuser Verlag, 2001, pp. 255–293.

[9] H. Schuster, C. Westermaier, and D. Schröder, "Non-identifier-based adaptive control for a mechatronic system achieving stability and steady state accuracy," in *Proc. Int. Conf. Control Appl. (CCA)*, Munich, Germany, 2006, pp. 1819–1824.

Analyzing the Robustness of Impulsive Synchronization Coupled by Linear Delayed Impulses

Anmar Khadra, Xinzhi Z. Liu, and Xuemin ShermanShen, *Senior Member, IEEE*

***Abstract*—In this technical note, a class of autonomous impulsive differential systems with linear delayed impulses is considered. Sufficient conditions required for this particular class of systems with varying and constant impulse durations to be equi-attractive in the large are obtained. These conditions are then applied to impulsively synchronize two coupled chaotic systems by using delayed impulses and a robustness analysis of the model is also provided. Simulation results are given to demonstrate the analytical results.**

***Index Terms*—Delay, equi-attractivity, impulsive synchronization.**

I. INTRODUCTION

The synchronization of coupled chaotic systems has become an active research area because of its potential applications to secure communication [7], [8]. A number of interesting communication security schemes based on chaos synchronization have been proposed. In these schemes, message signals are masked or modulated (encrypted) by using chaotic signals and the resulting encrypted signals are transmitted across a public channel. An identical synchronization between the chaotic systems at the transmitter and receiver ends is required for recovering the message signal [7]. Different types of synchronization techniques (some of which are robust to parameter mismatch and channel noise) have been developed in the literature [5], [7]. Synchrony was established in some of these studies using low dimensional chaotic systems and employing first and second Lyapunov techniques.

Most recently, another synchronization technique, called impulsive synchronization (IS), has been reported in [8]. The technique allows the coupling and synchronization of two or more chaotic systems by using only small synchronizing impulses. These impulses are samples of the state variables of the drive system at discrete moments that drive the response system. When equi-attractivity in the large of the synchronization error between the drive and the response systems is achieved, the two coupled systems are said to be synchronized. This technique has been applied to a number of chaos-based secure communication schemes which exhibit good performance as far as synchronization and security are concerned [8].

In general, transmission and sampling delays in communication security schemes based on IS are inevitable. Therefore, it is very crucial to examine the robustness of IS towards these two types of delay. There have been several attempts in the literature to study the existence, uniqueness, boundedness and stability of solutions of a particular class of delayed impulsive systems [1]. In fact, the stability of linear continuous-time systems possessing delayed discrete-time controllers in networked control systems have been also analyzed [2], [6], [9]. Such studies have been based on the notions of Lyapunov-Krasovskii functionals and Lyapunov-Razumikhin functions [3]. In this technical note, we investigate the stability of non-linear impulsive systems and IS in the presence of *linear delayed impulses*. By *linear delayed impulses* we mean that the mapping describing these impulsive moments (or discrete transitions) are linear in structure and dependent on delayed state variables. We derive sufficient conditions leading to synchronization when linear delayed impulses are applied. Our goal is to explore the sensitivity of IS to delayed impulses and obtain the maximum amount of delay the synchronization error could handle.

The remainder of this technical note is organized as follows. In Section II, a general impulsive system with linear delayed impulses resembling the structure of many chaotic systems is presented and the equi-attractivity of its zero-equilibrium solution is investigated. The analysis is developed for systems with both varying and constant impulse durations. In Section III, we present the motivation for constructing these systems and show several numerical simulations to illustrate the theory obtained in Section IV. Finally, in Section V, we summarize our results.

II. SYSTEMS WITH LINEAR DELAYED IMPULSES

Consider the impulsive system

$$\left\{\begin{array}{ll} \dot{\mathbf{x}} = A\mathbf{x} + \mathbf{\Phi}(t,\mathbf{x}), & t \neq \tau_i \\ \Delta\mathbf{x}(t) = B_i\mathbf{x}(t-r_i), & t = \tau_i \\ \mathbf{x}(t) = \boldsymbol{\phi}(t-t_0), & \end{array}\right\} \begin{array}{l} t > t_0 \\ \\ t_0 - r \leq t \leq t_0 \end{array} \tag{1}$$

where A is an $n \times n$ constant matrix, $\Delta\mathbf{x}(\tau_i) = \mathbf{x}(\tau_i^+) - \mathbf{x}(\tau_i^-)$, $\mathbf{x}(\tau_i^+) = \lim_{t-\tau_i^+}\mathbf{x}(t)$ and the moments of impulse satisfy $t_0 < \tau_1 < \tau_2 < \ldots < \tau_i < \ldots$ with $\lim_{i-\infty}\tau_i = \infty$. The function $\boldsymbol{\phi}(t-t_0)$ is an arbitrary differentiable initial function defined over $[t_0 - r, t_0]$ and r_i are delay constants satisfying $r := \max_i(r_i) \geq 0$, $i = 1, 2, \ldots$. Let k, k_i, $i = 1, 2, \ldots$, be a set of non-negative

Manuscript received May 26, 2008; revised September 29, 2008 and November 27, 2008. Current version published April 08, 2009. This work was supported in part by the Natural Sciences and Engineering Research Council of Canada. Recommended by Associate Editor S. Celikovsky.

A. Khadra is with Humboldt University of Berlin, Berlin D-10099, Germany (e-mail: khadraan@staff.hu-berlin.de).

X. Z. Liu and X. Shen are with the University of Waterloo, Waterloo, ON N2L 3G1, Canada (e-mail: xzliu@uwaterloo.ca; xshen@bbcr.uwaterloo.ca).

Digital Object Identifier 10.1109/TAC.2009.2013029